RAPID COMMUNICATIONS

PHYSICAL REVIEW B VOLUME 48, NUMBER 24 15 DECEMBER 1993-II

Evidence for martensitic fcc-bcc transition of thin Fe films on Cu(100)

K. Kalki, D. D. Chambliss, K. E. Johnson, R. J. Wilson, and S. Chiang
IBM Research Division, Almaden Research Center, 650 Harry Road, San Jose, California 95120
(Received 11 August 1993)

We report on the martensitic fcc-bcc phase transformation for Fe films grown at room temperature on Cu(100) in a thickness range from 10 to 20 monolayers. bcc(110) grains are highly elongated along $\langle 011\rangle_{fcc} \parallel [1\bar{1}1]_{bcc}$ and exhibit characteristic island growth with steps along $[001]_{bcc}$. The martensitic (i.e., sudden, collective, nondiffusive) transformation in the bulk of the film is demonstrated by STM topography, including the behavior of steps at grain boundaries and the presence of tilted surfaces arising from fcc-bcc interfaces.

In heteroepitaxial growth of thin films, structural transitions are driven by the lattice mismatch between the bulk stable phase and the substrate as the film changes with increasing coverage from its epitaxially stabilized structure into its bulk configuration.[1] In cases of small differences in lattice constant the misfit can be accommodated by introducing dislocations into the strained layers during growth. If, however, the bulk stable phase differs considerably in lattice constant and structure from the pseudomorphic film, the transition into the final bulk structure cannot be accomplished by small continuous changes of the lattice parameters.[2] In very thin films transformations which cause a complete change in structure have been investigated theoretically.[2] We describe here such a transformation, the martensitic transformation of a thin Fe film on Cu(100), which changes not only the surface morphology but also the crystal structure of already-grown layers close to the substrate. The orientation of bcc grains and the martensitic nature of the transformation are identified by the surface topography observed with scanning tunneling microscopy (STM).

The system Fe/Cu(100) has been studied extensively in order to relate structural details at various coverages to magnetic properties.[3–6] Fe grows at coverages below 14 monolayers (ML) nearly layer by layer, in an fcc-like structure which is pseudomorphic to the Cu(100) substrate.[7,5] However, the Fe films show a variety of reconstructions depending on coverage and film preparation[8,3,5,6] and, furthermore, reportedly tend to form dislocations upon sputtering or annealing at coverages $\geq$10 ML.[9] The fcc-Fe film is therefore only metastable, and at 20 ML has reached its bulk bcc structure. It has been established by transmission electron microscopy that at this coverage the Fe film has formed a polycrystalline bcc structure in a Pitsch orientational relationship between bcc crystallites and the Cu(100) substrate, namely, $(100)_{fcc} \parallel (110)_{bcc}$ and $\langle 011\rangle_{fcc} \parallel [1\bar{1}1]_{bcc}$ (Ref. 10) (i.e., one bcc close-packed direction is parallel to either in-plane fcc close-packed direction). Low-energy electron diffraction (LEED) and STM were used to confirm a transition to a bcc(110) surface, thus oriented, at thicknesses between 10 ML and 14 ML.[9] However, the mechanism for the structural transformation in these Fe films has not yet been described.

Martensitic transformations are common in bulk ferrous alloys. Grains of a bcc-like phase are formed from an fcc parent by the collective, nondiffusive movement of atoms in an "invariant plane" transformation of the lattice. This transformation is essentially a shear along a close-packed direction [Fig. 1(a)], combined with small expansions, contractions, and rotations because of the change in nearest-neighbor spacing; it results in approximately the Pitsch crystallographic relationship.[11] The transformation of part of a thin film may be envisioned as in Fig. 1(b). The collective motion forming a martensite grain leads to a highly anisotropic shape and to particular angles between the grain and its parent phase. These characteristics are all confirmed for the transformation reported here.

The UHV-STM apparatus used for these studies has been described in detail elsewhere.[12] The Cu(100) single crystal was cleaned by repeated cycles of Ar-ion sputtering and subsequent annealing to 600 °C until the C contamination was below the detection limit of the Auger electron spectroscopy (AES) system. Fe was evaporated from a pure Fe wire by electron bombardment. In order to keep the background pressure during deposition below 8×10^{-10} mbar the evaporator was extensively outgassed and enclosed in a liquid-nitrogen-filled cooling jacket. The deposition rate was monitored by an ion gauge in the Fe-vapor beam. All depositions have been carried out with the sample held at room temperature at a typical rate of 1 ML/80 s. The coverage was also

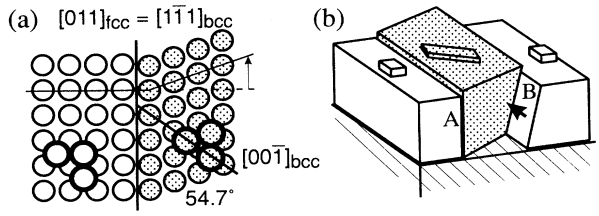

FIG. 1. Martensitic transformation. (a) Pitsch orientational relationship between a bcc-Fe(110) surface and pseudomorphic fcc-Fe(100) on Cu(100) (plan view). The fcc-bcc transformation consists mainly of a shear displacement (arrow) of atoms along one shared close-packed direction. Adatoms (heavy circles) are in fourfold-hollow sites on fcc(100), long bridge sites on bcc(110); favored steps on bcc(110) lie along $[001]_{bcc}$. (b) Thin-film martensitic grain. Martensite (shaded) forms by shear (arrow) plus expansions and/or contractions. One boundary with the fcc parent phase (white) is the invariant plane *A*, with no slip; slip between parent and martensite at *B* can be eliminated by a slip or twin boundary within the martensite grain. Shapes of islands grown on martensite reflect changed surface symmetry.

cross-checked by AES intensity ratios and comparison with respective literature data.[5]

Figure 2 shows the development of the structural transition in a series of STM images taken at different Fe coverages. The topography of the 4-ML film [Fig. 2(a)] reflects nearly layer-by-layer growth in accordance with medium-energy electron diffraction measurements[5] and exhibits isotropic island shapes with a weak preference for steps along the close-packed directions [011] and [01$\bar{1}$]. At 10 ML [Fig. 2(b)] the overall topography remains unchanged except for the appearance of narrow, slightly elevated stripes oriented along the close-packed $\langle 011\rangle_{fcc}$ directions, which we define as "needles." They end in a heavily distorted environment of the substrate visible as high islands partially surrounded by deep holes. The needles are 500–1000 Å long with a typical length to width ratio of 10–15. At a coverage of 14 ML [Fig. 2(c)], the film topography is dominated by long, narrow "ridges" typically 150 Å wide whose orientation is still along $\langle 011\rangle_{fcc}$. Such ridges may be several thousand Å long and typically extend up to another ridge in the perpendicular direction. They are raised somewhat, on average, against the neighboring surface, and exhibit a distinctive step and island structure. As shown below, these ridges are bcc-structured grains. However, about 30% of the film remains unchanged by the transformation, with topography comparable to the fcc-regions in the 10- and 4-ML film [arrow in Fig. 2(c)]. A LEED pattern of this 14-ML sample exhibits streaking along the close-packed fcc directions which agrees with the Pitch orientation. After 20-ML deposition the Fe film consists entirely of bcc grains, partly oriented along the $\langle 011\rangle_{fcc}$ directions. The now bcc surface of the Fe film has higher step density than the former epitaxial fcc film, characteristic for kinetic roughening observed in the growth of bcc material on bcc(110) substrates.[13]

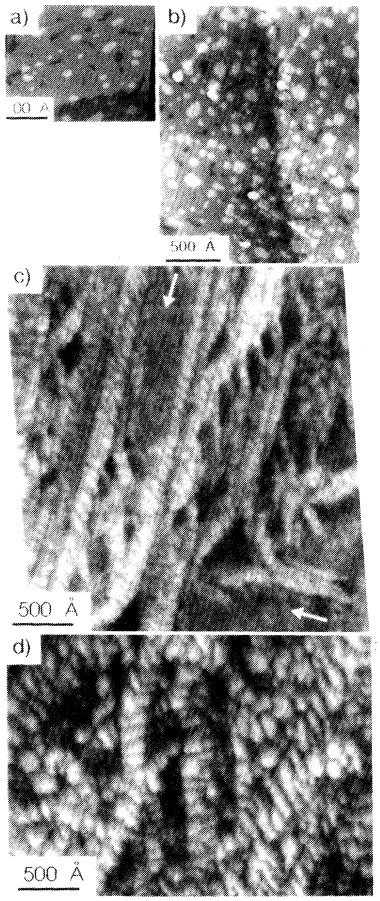

FIG. 2. Structural evolution with thickness for Fe films on Cu(100). STM images are presented in height-keyed gray scale; parallelogram shapes of some scanned regions result from thermal drift. (a) Pseudomorphic fcc structure at 4 ML. (b) "Needle" bcc grains in fcc matrix at 10 ML. (c) "Ridge" bcc grains at 14 ML. Arrows indicate remaining fcc regions. (d) Network of bcc grains at 20 ML.

To identify the structure and crystallographic orientation of the grains we examine the islands in different areas of the 14-ML Fe film in Fig. 3, showing a closeup view of parts of a ridge next to an fcc-like region. Cross sections along the horizontal scan direction in regions (I), (II), and (III) reveal step heights of 2.0±0.1 Å in (I) and (II), as expected for bcc-Fe(110) steps, and 1.7±0.1 Å in region (III) characteristic of fcc-Fe(100).[14] Furthermore, the islands in (I) exhibit an elongated shape, with preferred steps lying at an angle of 55° ± 3° to the bcc grain axis. This direction corresponds with $[001]_{bcc}$, the preferred step for growth of bcc material on bcc(110) substrates.[13,15] This directionality characterizes most ridges at 14 ML, with different island directions revealing the four bcc orientations generated by reflections in the (011) and (010) mirror planes of the substrate. Some bcc grains, region (II) in particular, have little or no growth on them, as discussed below. Another feature distinguishing the fcc and bcc phases is that the terraces on bcc grains are noticeably smoother, showing an rms roughness of 0.06±0.02 Å compared to 0.1±0.01 Å on the fcc terraces.[16] We also note that some

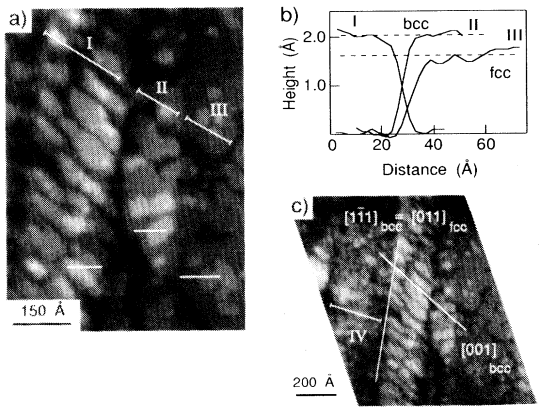

FIG. 3. Bcc grain structure at 14 ML. (a) Step and island structure of bcc and fcc regions. STM image is of an area contained within Fig. 2(c). Region (I) exhibits distinctive island shapes; step shapes in (II) and (III) are similar. (b) Step heights. Cross sections of regions (I), (II), and (III) along bars in (a) give bcc(110) steps in (I) and (II), and fcc(100) steps in (III). (c) Crystallographic directions. Grains are oriented along $\langle 011\rangle_{fcc} = [1\bar{1}1]_{bcc}$ and bcc islands lie along $[001]_{bcc}$. Region (IV), with high step density, contains tilted planes.

of the ridges in the 14-ML sample [cf. Fig. 3(a)] are wedge shaped: the two fcc/bcc interfaces are not exactly parallel but make an angle of ~3°.

"Needle" grains in the 10-ML film are much smaller, and distinct islands indicative of the bcc type growth as in the 14-ML film have not yet developed. The appearence of the needles is therefore correlated with the onset of the transformation around 10 ML thickness. Several aspects of the grain's geometry at 10 ML show their similarity to the ridges at 14 ML. First, needles are oriented along the $\langle 011\rangle_{fcc}$ directions. Second, islands on needles exhibit the same step height as found in the bcc grains of the 14-ML film, namely, 2.0 Å. Third, we find a similar wedge-shaped outline of the needle [Fig. 4(a)]. Finally, the rms roughness on the needles and in the surrounding region equals the roughness of bcc and fcc terraces, respectively, at 14 ML. The needles therefore have the same bcc structure and grain orientation as the ridges in the 14-ML film. We mention that this kind of structural determination was not possible for a small subset of the needles with a different structure, resembling the "protruding streaks" reported by Wuttig *et al.*[9] These have a constant width of 40 Å and are symmetric about their axis, and while the size and symmetry rule out a simple dislocation structure neither can a bcc structure be demonstrated.[17]

The sudden, collective, bulklike nature of the transformation is evident in bcc-fcc boundaries such as that between regions (II) and (III) in Fig. 3(a). The step edges bounding islands and holes are nearly continuous across the boundary, and the near straightness of the boundary is unaffected by the surface steps. These characteristics typical of 14-ML ridges hold also at 10 ML, as seen in Fig. 4(a). Thus the transition must be in the bulk of the film, involving many layers. For comparison, it is characteristic of surface reconstructions observed with the STM that steps exert strong influence on the domain structures, and are often themselves the dominant domain boundaries. Here, the grain boundaries are unaffected by steps, as expected for a boundary determined in the bulk. Furthermore, the step topography of the starting surface is largely preserved by the transformation, as can be seen in all needles at 10 ML and some grains at 14 ML [e.g., region (II)]. This implies a rapid, collective motion: in a transformation by diffusional atomic rearrangement, all memory of the previous step and island structure would be lost. Only on grains transformed just before, or after, the end of deposition is the preservation of original steps evident. From this it is clear that all of region (II) was transformed nearly simultaneously, at least as measured against the very slow "clock" of deposition and aggregation. In the collective shear of a martensitic transformation, steps remain intact but are changed in height and direction, as can be seen in Fig. 1(a). While the step height is readily measured, the direction change is difficult to observe because long, straight step segments are uncommon in the parent fcc phase, and because any post-transformation aggregation of Fe changes step shapes. Nonetheless, some steps in Fig. 4(a) appear to be bent at the boundary by the transformation.

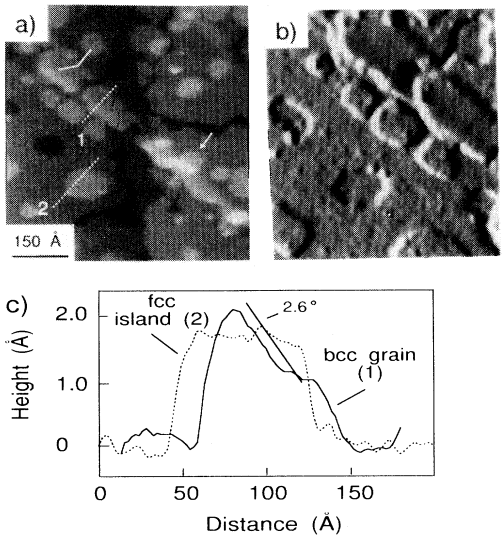

FIG. 4. "Needle" bcc grain at 10 ML. (a) Shape of grain. Grain crosses a step of the substrate, and exhibits a wedge shape with narrow end at lower right and an angle 3°. Arrow marks island at which step height was measured (using close-up image) at 2.0 Å atop needle and 1.7 Å on fcc portion. Bent line indicates expected bending of close-packed fcc step by martensitic transformation. Dashed lines are locations of sections in (c). (b) Differentiated view dz/dx of section of (a) near upper right. "Needle" surface has smaller rms roughness (0.06±0.02 Å) than surrounding regions (0.10±0.01 Å). (c) Cross sections of bcc needle (1) and fcc island (1). Needle is tilted, and smoother than fcc region.

The buried interfaces between the bcc grains and the fcc parent presumably adopt structures and orientations that minimize the interface energy, within kinetic limitations. In bulk martensites the interface planes deviate from low-index planes, typically by several degrees, to accommodate the mismatch in nearest-neighbor spacing between parent and martensite ($a_{n\text{-}n}$ is ~3% smaller in bcc Fe than in fcc Cu). Steps on a tilted interface can provide lower-energy locations, or eliminate the need, for matching dislocations between the fcc and bcc nearest-neighbor rows. Such tilted interfaces may explain the ~3° full angle characteristic of the wedge-shaped grains in our sample. More important, tilted buried interfaces explain the many parts of our samples where bcc regions are flat over areas $\sim(30\ \text{Å})^2$ but are unambiguously tilted several degrees away from $(100)_{fcc}$. A typical 10-ML needle is tilted ≈3° about its long axis (Fig. 4). Similar tilt angles are observed near grain boundaries in the 14-ML film. Some highly stepped regions like (IV) in Fig. 3(c) appear on closer examination to contain many narrow, tilted terraces. These various small-angle tilts cannot be explained as a change in surface structure alone, but are reasonable if tilted boundaries of a bulklike grain are assumed. For comparison, a boundary between close-packed planes $(111)_{fcc} \parallel (011)_{bcc}$ with $[01\bar{1}]_{fcc} \parallel [1\bar{1}1]_{bcc}$ would account for a tilt angle of 5.3° between exposed $(110)_{bcc}$ and $(100)_{fcc}$ surfaces. On the other hand, some bcc areas exhibit no significant tilt, as for most of regions (I) and (II). This suggests that an interface $(110)_{bcc} \parallel (100)_{fcc}$ may also be energetically pos-

sible. In region (II) of Fig. 3, typical of such areas, the transformation raises the average surface level by 1.1± 0.1 Å which is neither an fcc nor a bcc step height. This height change, if uniform over the entire grain, would imply a volume increase of ~4% in the grain, comparable to the expected fcc-bcc volume change for Fe.

While the combined shear and contraction-expansion of a martensitic transformation leaves fixed the long, smooth, nearly close-packed sides (the "invariant planes"), it can involve large compressive or tensile strain at the narrow grain ends. This accounts for the narrowness of these grains, which minimizes the strained volume; the apparent tendency for 14-ML grains to have grown indefinitely (up to a collision with another grain) may maximize the ratio of transformed volume to highly strained end volume. High end stress is also presumably the source of the distorted features seen at the tips of the needles in Fig. 2(b). It is not clear why these defects are much larger at the wider ends of the needles. Since these features are not observed except at needle ends, it is unlikely that they are formed first and then act as nucleation sites for the transformation; they appear to be effect rather than cause. We note that the surface topography offers no evidence of any other nucleating defects, and in particular the ends of needle grains do not appear correlated with the steps of the substrate.

The disordered roughness of fcc regions in films described here, which goes away upon a transition to bcc, suggests an instability of the fcc-Fe(100) surface against local structural relaxation. Such an instability is also manifest in the surface reconstructions observed at much lower coverage (1–3 ML).[8,3,5] Indeed, their LEED patterns are best explained by in-plane shear structures,[8] which may be surface analogs of the martensitic transformation seen here. LEED streaking often seen at intermediate thicknesses also suggests in-plane shear, though in a disordered structure. Thus one may suspect a tendency to assume a bcc-like local bond geometry at the surface, even before the martensitic transformation produces bulklike bcc grains. Such in-plane displacements at the surface would presumably play a role in the different magnetic behavior reported for the surface and bulk of thin Fe films.[18] An instability against shear distortion should also appear as a phonon softening near the Brillouin zone edge, similar to that reported already[8] but with an in-plane transverse polarization that is more difficult to observe experimentally.

In conclusion, the topographic features of these Fe films—the size, shape, and orientation of grains, the island growth on bcc grains, the rapidity of the transformation, and the tilted planes—all indicate the martensitic nature of the fcc-bcc transition. Such a transformation should not be unexpected, since it is fundamental to many properties of Fe and ferrous alloys. Its observation in such thin films raises questions about structural transformations in other thin metal films. For example, the common assumption that buried layers will retain their structure unless subjected to severe chemical or mechanical stress is clearly not true for the collective motion in the bulk that occurs here. Explorations of the structural complexity possible in epitaxial thin films are crucial to understanding their special properties.

We have become aware of similar data and conclusions in Ref. 19. Some differences in detail may arise from the difference between a single deposition step (present work) and deposition increments separated by STM data acquisition (Ref. 19).

We are grateful to J. Giergiel and A. Roytburd for stimulating discussions, and to the F. Lynen program of the A.v. Humboldt Foundation and the Office of Naval Research (N00014-89-C-0099) for support.

[1] M. Thikhov and E. Bauer, Surf. Sci. **232**, 73 (1990).
[2] R. Bruinsma and A. Zangwill, J. Phys. (Paris) **47**, 2055 (1986).
[3] D.P. Pappas, K.-P. Kämper, and H. Hopster, Phys. Rev. Lett. **64**, 3179 (1990).
[4] K.E. Johnson, D.D. Chambliss, R.J. Wilson, and S. Chiang (unpublished).
[5] J. Thomassen, B. Feldmann, and M. Wuttig, Surf. Sci. **264**, 406 (1992).
[6] F. Scheurer, R. Allenspach, P. Xhonneux, and E. Courtens, Phys. Rev. B **48**, 9890 (1993).
[7] K.E. Johnson, D.D. Chambliss, R.J. Wilson, and S. Chiang, J. Vac. Sci. Technol. A **11**, 1654 (1993).
[8] W. Daum, C. Stuhlmann, and H. Ibach, Phys. Rev. Lett. **60**, 2741 (1988).
[9] M. Wuttig, B. Feldmann, J. Thomassen, F. May, H. Zillgen, A. Brodde, H. Hannemann, and H. Neddermeyer, Surf. Sci. **291**, 14 (1993).
[10] J. Koike and M. Nastasi, in *Evolution of Thin Films and Surface Microstructure*, edited by C.V. Thompson, J.Y. Tsao, and D.R. Srilovitz, MRS Symposia Proceedings No. 202 (Materials Research Society, Pittsburgh, 1991), p. 13.
[11] C.M. Wayman, in *Physical Metallurgy*, 3rd ed., edited by R.W. Cahn and P. Haasen (Elsevier, Amsterdam, 1983), pp. 1031–1074.
[12] S. Chiang, R.J. Wilson, Ch. Gerber, and V.M. Hallmark, J. Vac. Sci. Technol. A **6**, 386 (1986).
[13] H. Fritzsche and U. Gradmann, in *Common Themes and Mechanisms of Epitaxial Growth*, edited by P. Fuoss, D.W. Kisker, J. Tsao, A. Zangwill, and T.F. Kuech, MRS Symposia Proceedings No. 312 (Materials Research Society, Pittsburgh, 1993), p. 321.
[14] The error given here results from topographic roughness and does not include a 5% uncertainty in absolute calibration, which does not affect the comparison of fcc(100) and bcc(110) steps.
[15] P. Hahn, J. Clabes, and M. Henzler, J. Appl. Phys. **51**, 2079 (1988).
[16] Instrumental factors (such as noise and incomplete background removal) add about 0.02–0.04 Å in quadrature to the actual rms roughness, but this offset should be the same for fcc and bcc regions in a given image. Thus an ideal measurement would yield smaller absolute roughnesses and a somewhat larger ratio between fcc and bcc.
[17] D.D. Chambliss, K. Kalki, and K.E. Johnson (unpublished).
[18] J. Thomassen, F. May, B. Feldmann, M. Wuttig, and H. Ibach, Phys. Rev. Lett. **69**, 3831 (1992).
[19] J. Giergiel, J. Kirschner, J. Landgraf, J. Shen, and J. Woltersdorf (unpublished).

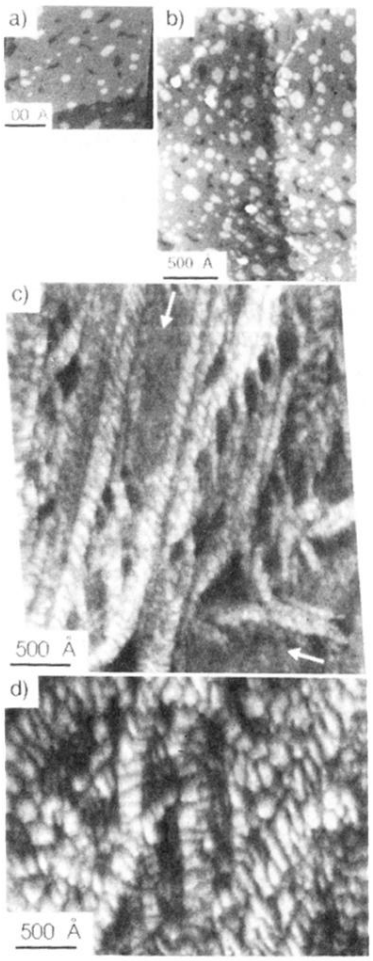

FIG. 2. Structural evolution with thickness for Fe films on Cu(100). STM images are presented in height-keyed gray scale; parallelogram shapes of some scanned regions result from thermal drift. (a) Pseudomorphic fcc structure at 4 ML. (b) "Needle" bcc grains in fcc matrix at 10 ML. (c) "Ridge" bcc grains at 14 ML. Arrows indicate remaining fcc regions. (d) Network of bcc grains at 20 ML.

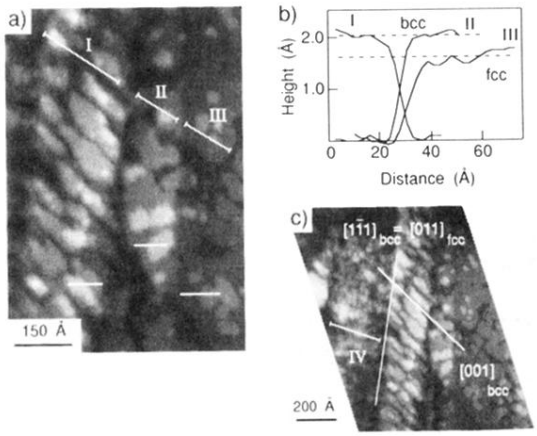

FIG. 3. Bcc grain structure at 14 ML. (a) Step and island structure of bcc and fcc regions. STM image is of an area contained within Fig. 2(c). Region (I) exhibits distinctive island shapes; step shapes in (II) and (III) are similar. (b) Step heights. Cross sections of regions (I), (II), and (III) along bars in (a) give bcc(110) steps in (I) and (II), and fcc(100) steps in (III). (c) Crystallographic directions. Grains are oriented along $\langle 011 \rangle_{\mathrm{fcc}} = [1\bar{1}1]_{\mathrm{bcc}}$ and bcc islands lie along $[001]_{\mathrm{bcc}}$. Region (IV), with high step density, contains tilted planes.

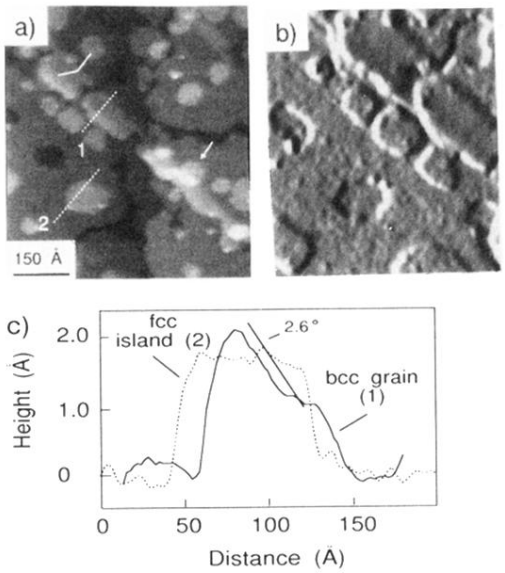

FIG. 4. "Needle" bcc grain at 10 ML. (a) Shape of grain. Grain crosses a step of the substrate, and exhibits a wedge shape with narrow end at lower right and an angle 3°. Arrow marks island at which step height was measured (using close-up image) at 2.0 Å atop needle and 1.7 Å on fcc portion. Bent line indicates expected bending of close-packed fcc step by martensitic transformation. Dashed lines are locations of sections in (c). (b) Differentiated view dz/dx of section of (a) near upper right. "Needle" surface has smaller rms roughness (0.06 ± 0.02 Å) than surrounding regions (0.10 ± 0.01 Å). (c) Cross sections of bcc needle (1) and fcc island (1). Needle is tilted, and smoother than fcc region.